Silaffin 1A$_1$: Insights to the Processes of Tailored Silica Precipitation

Fanny Kozak[1,2], Fabian Daus[3], Dörte Brandis[1,2], Armin Geyer[3], Christian W. F. Becker[1], Dennis Kurzbach[1]

[1]Institute of Biological Chemistry, Faculty of Chemistry, University of Vienna, Währingerstraße 38, 1090 Vienna, Austria.
[2]University of Vienna, Doctoral School of Chemistry (DoSChem), Währingerstraße 42, 1090 Vienna, Austria
[3]Faculty of Chemistry, Philipps-Universität Marburg 35032, Marburg, Germany

E-Mail: fanny.kozak@univie.ac.at,
Find us at: www.Kurzbach-group.univie.ac.at

https://doi.org/10.17952/37EPS.2024.P1299

1) Introduction

The variety and intricate beauty of diatom algaes' typical silica shells inherently demands to pose the question of how these organisms are capable of shaping silica from the intrinsically low silicic acid concentration in seawater. Further than the urge to understand **biomineralization** on a deeper level, the ability to develop **tailored silica particles** allows for new approaches to drug delivery and provides a further step in rational materials design. Peptide Silaffin 1A$_1$, isolated from marine diatom species ***Cylindrotheca fusiformis***, is one of the molecules enabling controlled silica precipitation in the presence of positively charged ions.[1] Still, the mechanism leading to controlled silica precipitation under mild conditions is scarcely understood.

A) Synthetic Silafin1A$_1$ ($_{syn}$Sil1A$_1$)

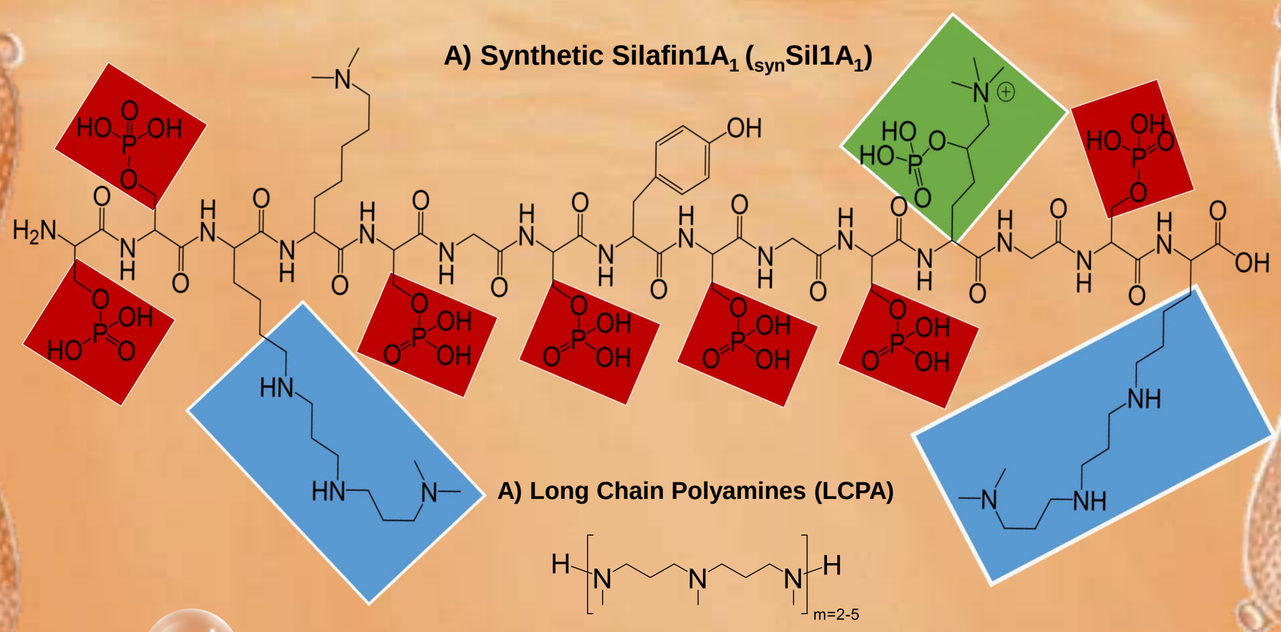

A) Long Chain Polyamines (LCPA)

3) Synthetic Silafin1A$_1$

Synthetic Silafin1A$_1$ ($_{syn}$Sil1A$_1$) differs from its natural scaffold by the homogeneous length of the polyamine **post-translational modifications**. Still, to yield homogeneously sized particles, adding **long-chain polyamides** LCPA) is necessary. Structures are shown in Figure A). This facilitates **supramolecular assembly** necessary for the precipitation event. Depending on the conditions chosen, influence is taken on the morphology of the precipitate [2]. This process is closely related to similar biomineralization processes, which are debated to not follow the classical scheme of nucleation, But rather to form **prenucleation species**, which are subject to growth until sizes susceptible for solid formation are formed [3] (Fig.B)

2) Diatoms

Their intricate silica shells served as inspiration for designing mimetic peptides and sparked further interest in unraveling biomineralisation processes. Shown: *Mastogloia binotata* (Grun.) [4,]

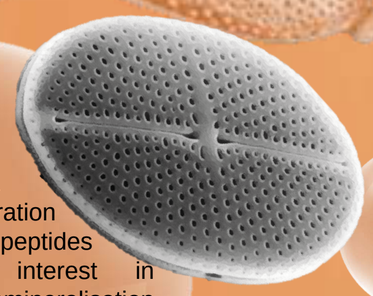

C) ^{1}H-^{31}P Correlation Spectra

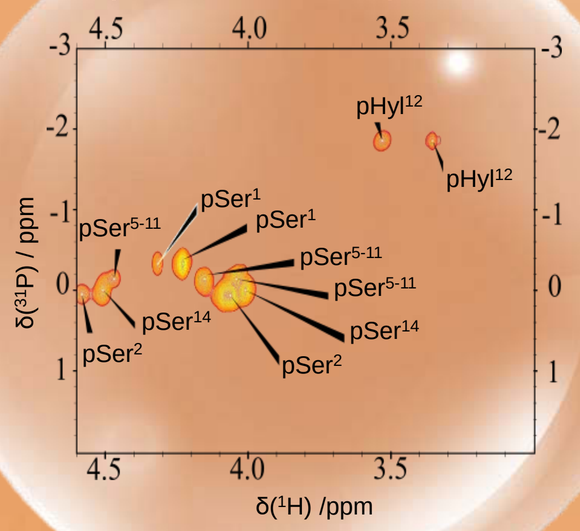

E) ^{31}P Relaxation Rates

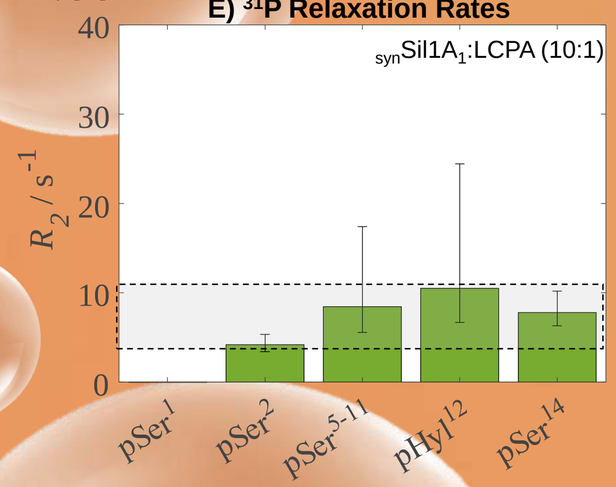

F) ^{1}H- ^{31}P Relaxation Rates

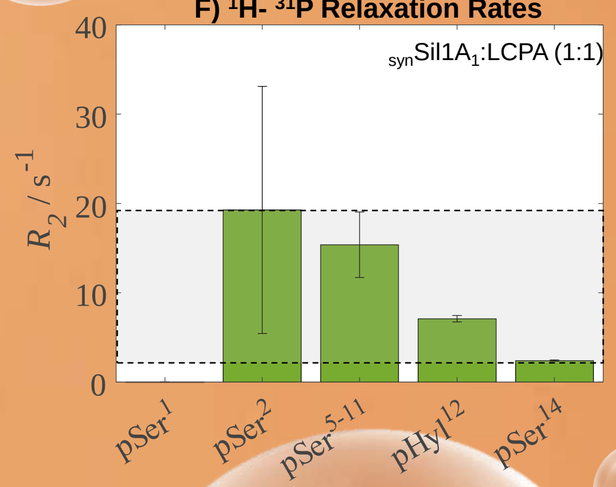

D) ^{1}H-^{31}P CPMG Pulsesequence

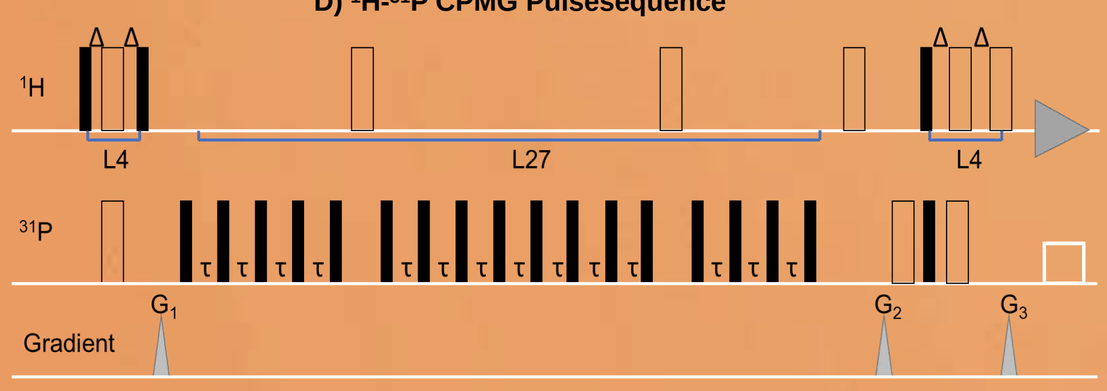

4) ^{1}H-^{31}P CPMG Pulsesequence

To allow for residue resolution, we detected the **post-translational phosphorylations** by a specifically designed pulse sequence. Therefore, we traced ^{1}H-^{31}P T_2 relaxation rates in different conditions. Pulse sequence, as well as extracted relaxation rates (E& F) and ^{1}H ^{31}P correlation spectrum, can be seen in Figure C+D. The sequence contains an additional CPMG train during the magnetization transfer as devised by Luy and Marino [5] for **enhanced sensitivity** (L4) combined with a traditional Carr-Purcell-Meiboom-Gill sequence for T_2 determination.

5) ^{1}H-^{31}P CPMG

Figure E and F show the changes depending on LCPA additive concentration. Upon adding different concentrations of LCPA, we observe an increase in R2 rates with increasing LCPA availability. This points towards decreasing mobility and indicates, combined with DOSY-data (not shown) **supramolecular assemblies** varying in structure, depending on additive presence.

G)

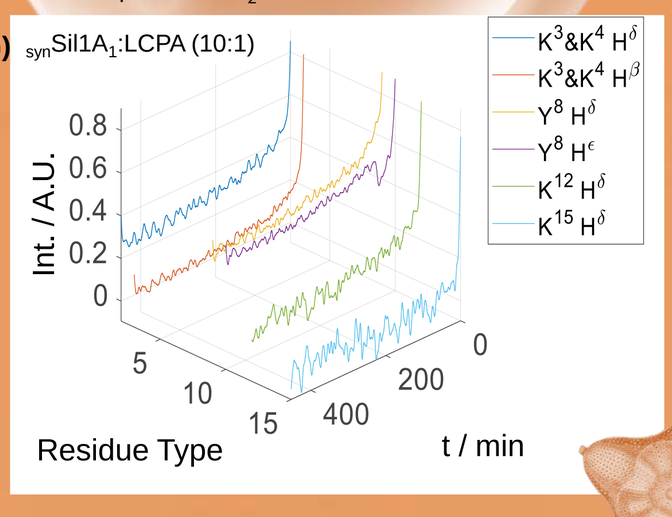

6) Real-time Precipitation Assay

The precipitation is triggered by the addition of silicic acid to the formed assemblies. To observe the influence of different LCPA concentration in the precipitation event, we traced the change in intensity by real-time 1D proton spectroscopy (Figure G and H). **Kinetic constants** were extracted by **exponential fitting** and can be seen in figure G) for $_{syn}$Sil1A$_1$:LCPA (10:1) and in figure H) for $_{syn}$Sil1A$_1$:LCPA (1:1).

The extracted kinetic constants are shown in the respective panels below, showing different involvement of different residues, depending on the concentration of LCPA. These differences in kinetic involvement and in the dynamic behavior of the R_2 rates, are conserved in the morphology of the precipitate. By **Scanning Electron Microscopy** (SEM), we observed smaller particle sizes for $_{syn}$Sil1A$_1$:LCPA (10:1) (Figure I) than for $_{syn}$Sil1A$_1$:LCPA (1:1) (shown in Figure K). Concluding, bridging further the gap between **liquid precursors** and precipitate, insights contribute to a deeper understanding of the events leading to bio(mimetic) mineralization. [6,7]

H)

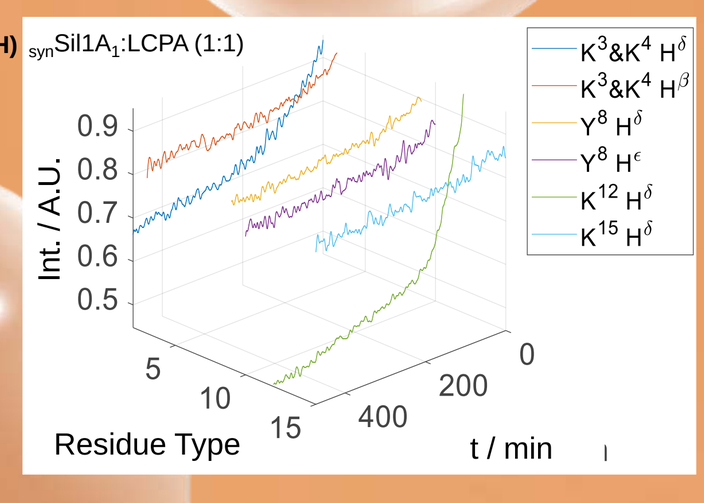

G) Real-time Assay, Kinetic Constants

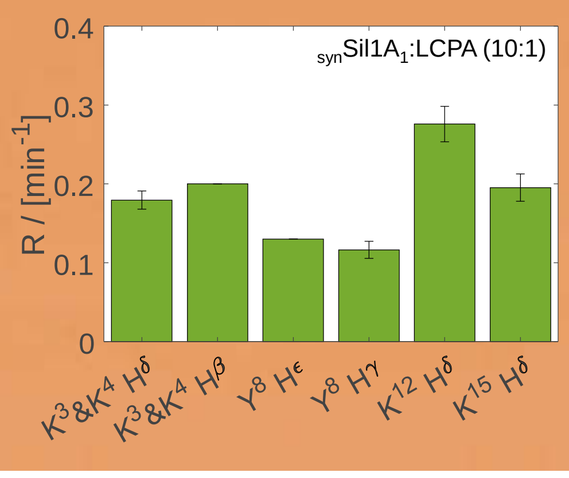

I)

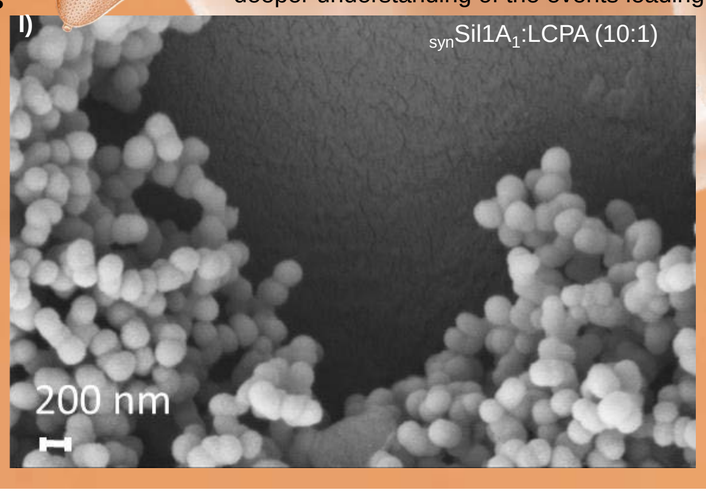

K)

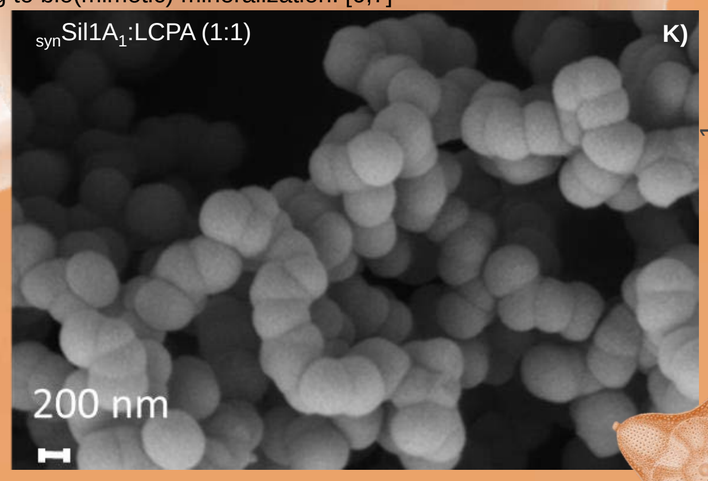

H) Real-time Assay, Kinetic Constants

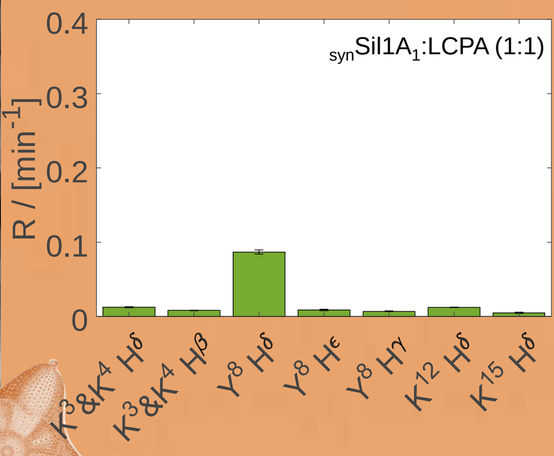

[1] Lechner CC, Becker CFW. *J Pept Sci* **2014**;20:152–8.
[2] Daus F, Xie X, Geyer A. *Org Biomol Chem* **2022**;3:3387–96.
[3] Gebauer D, Völkel A, Cölfen H. *Science* (80-) **2008**;322:1819–22.
[4] A. Falciatore, C. Bowler, *Annu. Rev. Plant Biol.* **2002**, *53*, 109–130.
[5] B. Luy, J. P. Marino, *J. Am. Chem. Soc.* **2001**, *123*, 11306–11307.
[6] F. Kozak, D. Brandis, C. Pötzl, L. M. Epasto, D. Reichinger, D. Obrist, H. Peterlik, A. Polyansky, B. Zagrovic, F. Daus, A. Geyer, C. F. Becker, D. Kurzbach, *Adv. Sci*. **2024**, 2401239.
[7] J. Strobl, F. Kozak, M. Kamalov, D. Reichinger, D. Kurzbach, C. F. Becker, *Adv. Mater*. **2023**, 35, 2207586.

INSTITUT FÜR BIOLOGISCHECHEMIE
erc European Research Council Established by the European Commission
FWF Der Wissenschaftsfonds.
universität wien